

Figure 3. Pressure versus composition diagram for the carbon dioxide (1)-*n*-propylcyclohexane (2) system: (Δ) this work at 313.1 K; (X) this work at 393.2 K; (∇) this work at 472.8 K; (\square) from Kim et al. (12) at 315.4 K; (\diamond) from Kim et al. (12) at 392.7 K; (+) from Kim et al. (12) at 474.6 K.

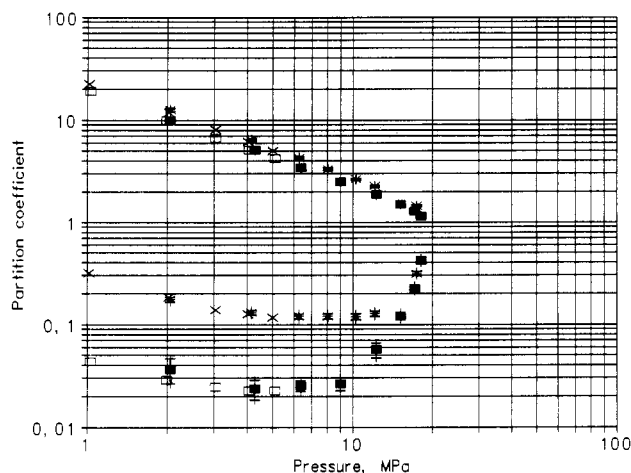


Figure 4. Partition coefficient versus pressure diagram for the carbon dioxide (1)-*n*-propylcyclohexane (2) system: (\blacksquare) this work at 393.2 K (indicated with error bars); (※) this work at 472.8 K (indicated with error bars); (\square) from Kim et al. (12) at 392.7 K; (X) from Kim et al. (12) at 474.6 K.

Acknowledgment

We are grateful to the members of the *K* value Screening Committee, especially to Dr. H. Kistenmacher, for encouragement and advice, and we thank A. Chareton, A. Valtz, P. Alali, C. Lafeuil, F. Fontalba, J. Destève, and D. Legret for their contribution.

Registry No. N_2 , 7727-37-9; CO_2 , 124-38-9; H_2S , 7783-06-4; propylcyclohexane, 1878-92-8; toluene, 108-88-3; *m*-xylene, 108-38-3; mesitylene, 108-67-8; propylbenzene, 103-65-1.

Literature Cited

- (1) Richon, D.; Laugler, S.; Renon, H. *J. Chem. Eng. Data* **1991**, *36*, 104.
- (2) Prausnitz, J. M.; Keeler, R. N. *AIChE J.* **1961**, *7*, 399.
- (3) Renon, H.; Laugler, S.; Schwartzentruber, J.; Richon, D. *Fluid Phase Equilib.* **1989**, *51*, 285.
- (4) Legret, D.; Richon, D.; Renon, H. *AIChE J.* **1981**, *27*, 203.
- (5) Figlière, P.; Hom, J. F.; Laugler, S.; Renon, H.; Richon, D.; Szwarc, H. *AIChE J.* **1980**, *26*, 872.
- (6) Fontalba, F.; Richon, D.; Renon, H. *Rev. Sci. Instrum.* **1984**, *55*, 944.
- (7) Laugler, S.; Richon, D. *Rev. Sci. Instrum.* **1986**, *57*, 469.
- (8) Laugler, S.; Legret, D.; Destève, J.; Richon, D.; Renon, H. GPA Research Report RR-59; Gas Processors Association: Tulsa, OK, 1982.
- (9) Laugler, S.; Alali, P.; Valtz, A.; Chareton, A.; Fontalba, F.; Richon, D.; Renon, H. GPA Research Report RR-75; Gas Processors Association: Tulsa, OK, 1984.
- (10) Chareton, A.; Valtz, A.; Lafeuil, C.; Laugler, S.; Richon, D.; Renon, H. GPA Research Report RR-101, Gas Processors Association: Tulsa, OK, 1986.
- (11) Timmermans, J. *Physico-chemical Constants of Pure Organic Compounds*; Elsevier: Amsterdam, 1965.
- (12) Kim, H.; Lin, H.-M.; Chao, K. C. *AIChE Symp. Ser.* **1985**, *81* (244), 96.

Received for review January 22, 1991. Revised October 21, 1991. Accepted October 21, 1991. We are grateful to the Gas Processors Association for financial support.

Phase Compositions, Viscosities, and Densities for Aqueous Two-Phase Systems Composed of Polyethylene Glycol and Various Salts at 25 °C

Steven M. Snyder, Kenneth D. Cole,* and David C. Szlag

National Institute of Standards and Technology, 325 Broadway, Boulder, Colorado 80303

Phase diagrams of aqueous two-phase systems composed of polyethylene glycol and various salt solutions were measured. The densities and viscosities of these phase systems were also measured. Polyethylene glycol was used with three average molecular masses of 1000, 3350, and 8000. The salts used were magnesium sulfate, sodium sulfate, sodium carbonate, ammonium sulfate, and potassium phosphate. Phase diagram data, as well as the densities and viscosities of the phases, were measured at 25 °C.

Introduction

Liquid-liquid extraction utilizing aqueous two-phase systems (ATPS) has been used to separate and purify biological products

from the complex mixtures in which they are produced (1, 2). Data on the composition and properties of phase systems are necessary for the design of ATPS extraction processes. Phase-diagram data are also necessary for the development of models that predict phase partitioning (3-6).

In this work, a comprehensive set of densities, viscosities, and phase compositions of ATPS composed of various polyethylene glycol (PEG) masses and salts were measured at 25 °C. A previous technique has been used to determine compositions of polymer-polymer systems utilizing measurements of optical rotation and refractive index (1, 2, 7, 8). However the PEG-salt systems have little or no optical activity. Potassium phosphate-PEG systems can be determined by titration (1); however, this method does not apply to the other salts used. Therefore, the gravimetric method of determining phase composition described by Stewart and Todd (9) was used and

Table I. Compositions and Physical Properties of Magnesium Sulfate-PEG Systems

system	total system				top phase				bottom phase					
	PEG/ (mass %)	salt/ (mass %)	water/ (mass %)	density/ (kg/m ³)	PEG/ (mass %)	salt/ (mass %)	water/ (mass %)	viscosity/ (Pa-s)	density/ (kg/m ³)	PEG/ (mass %)	salt/ (mass %)	water/ (mass %)	viscosity/ (Pa-s)	density/ (kg/m ³)
	PEG 1000													
A	14.0	9.5	76.5	1086.9	30.6	3.3	66.1	0.0065	1086.9	6.3	13.2	80.5	0.0033	1156.1
B	14.5	10.0	75.5	1082.2	33.5	3.1	63.4	0.0078	1082.2	3.8	14.6	81.6	0.0033	1165.7
C	15.0	10.5	74.5	1079.7	36.1	3.1	60.8	0.0085	1079.7	2.6	15.7	81.7	0.0034	1184.5
D	15.5	11.0	73.5	1079.6	37.8	3.1	59.1	0.0097	1079.6	2.0	16.5	81.5	0.0035	1198.4
	PEG 3350													
E	12.3	7.9	79.9	1068.4	25.4	3.1	71.5	0.0126	1068.4	4.8	12.2	83.1	0.0023	1126.0
F	13.1	8.9	77.9	1068.9	29.2	2.6	68.2	0.0177	1068.9	4.5	13.9	81.7	0.0023	1142.9
G	14.0	9.8	76.2	1072.5	32.8	2.5	64.7	0.0227	1072.5	5.1	14.2	80.7	0.0025	1161.4
H	14.7	10.5	74.8	1076.0	34.4	2.4	63.2	0.0238	1076.0	4.4	15.2	80.4	0.0025	1167.2
	PEG 8000													
I	12.0	8.0	80.0	1064.8	25.2	3.8	71.0	0.0418	1064.8	3.8	12.5	83.7	0.0020	1127.5
J	14.0	9.5	76.5	1070.7	32.3	2.6	65.1	0.0768	1070.7	0.8	14.5	84.7	0.0024	1161.0
K	14.5	10.0	75.5	1072.3	33.5	2.3	64.2	0.0941	1072.3	0.7	15.1	84.3	0.0024	1172.2
L	15.0	10.5	74.5	1073.7	35.2	2.2	62.6	0.1060	1073.7	0.8	15.9	83.3	0.0027	1181.4
M	15.5	11.0	73.5	1075.7	38.2	1.7	60.1	0.1220	1075.7	1.2	16.7	82.2	0.0030	1191.6

Table II. Compositions and Physical Properties of Potassium Phosphate-PEG, pH 8.0, Systems

system	total system				top phase				bottom phase					
	PEG/ (mass %)	salt/ (mass %)	water/ (mass %)	density/ (kg/m ³)	PEG/ (mass %)	salt/ (mass %)	water/ (mass %)	viscosity/ (Pa-s)	density/ (kg/m ³)	PEG/ (mass %)	salt/ (mass %)	water/ (mass %)	viscosity/ (Pa-s)	density/ (kg/m ³)
	PEG 1000													
A	16.1	10.0	73.9	1091.4	22.7	6.8	70.5	0.0053	1091.4	5.0	16.0	79.0	0.0019	1164.1
B	17.9	10.5	71.6	1086.2	28.9	5.0	66.1	0.0069	1086.2	2.8	18.7	78.5	0.0017	1182.3
C	20.0	11.4	68.6	1087.6	36.1	3.5	60.4	0.0097	1087.6	2.1	21.6	76.3	0.0018	1209.0
D	22.0	12.3	65.7	1089.2	39.1	3.1	57.8	0.0130	1089.2	1.6	24.0	74.4	0.0020	1237.1
	PEG 8000													
E	12.1	7.7	80.2	1071.8	21.7	4.4	73.9	0.0199	1071.8	1.9	11.5	86.7	0.0013	1103.2
F	13.9	7.7	78.4	1072.5	24.6	3.9	71.5	0.0273	1072.5	1.6	12.4	86.1	0.0013	1112.4
G	16.1	10.0	73.9	1079.3	34.6	2.6	62.9	0.0771	1079.3	1.6	16.3	82.1	0.0014	1152.3
H	17.9	10.8	71.3	1082.5	38.1	2.2	59.7	0.1050	1082.5	2.3	18.3	79.4	0.0015	1172.8
I	20.0	11.6	68.4	1085.2	41.2	1.8	57.0	0.1480	1085.2	3.0	20.6	76.4	0.0017	1197.6
J	21.9	12.3	65.8	1088.5	44.4	1.6	54.0	0.2020	1088.5	2.0	23.1	74.9	0.0018	1223.9

Table III. Compositions and Physical Properties of Sodium Carbonate-PEG Systems

system	total system				top phase				bottom phase					
	PEG/ (mass %)	salt/ (mass %)	water/ (mass %)	density/ (kg/m ³)	PEG/ (mass %)	salt/ (mass %)	water/ (mass %)	viscosity/ (Pa-s)	density/ (kg/m ³)	PEG/ (mass %)	salt/ (mass %)	water/ (mass %)	viscosity/ (Pa-s)	density/ (kg/m ³)
A	12.7	7.0	80.3	17.9	5.8	76.3	0.0047	1083.5	7.6	10.1	82.3	0.0029	1104.7	
B	9.9	10.9	79.2	34.2	2.1	63.7	0.0093	1076.3	2.0	13.7	84.2	0.0020	1141.7	
C	13.6	10.5	75.9	38.5	1.3	60.2	0.0114	1078.3	1.5	14.5	84.0	0.0021	1157.9	
D	11.9	11.9	76.3	39.4	1.8	58.8	0.0129	1080.0	1.1	16.3	82.6	0.0022	1167.6	
E	14.9	12.9	72.1	45.9	1.0	53.1	0.0176	1085.4	1.9	17.8	80.3	0.0029	1197.0	
PEG 1000														
F	14.0	10.9	75.1	37.5	4.5	58.0	0.0483	1081.9	0.8	14.4	84.8	0.0022	1156.0	
G	16.1	11.9	72.0	43.2	4.3	52.5	0.0620	1087.2	0.5	16.5	83.0	0.0026	1178.7	
H	20.0	14.0	66.0	50.5	3.4	46.2	0.0933	1094.2	1.5	20.3	78.2	0.0038	1225.0	
PEG 3350														
I	11.7	5.6	82.7	25.9	2.2	71.9	0.0325	1063.9	0.5	8.5	91.1	0.0014	1084.2	
J	19.0	6.0	75.0	34.9	2.1	63.0	0.0850	1072.5	0.5	11.7	87.8	0.0017	1116.3	
K	8.8	12.1	79.1	42.9	0.8	56.3	0.1670	1081.4	0.5	15.0	84.5	0.0021	1147.2	
L	10.3	14.3	75.5	48.0	0.1	51.8	0.2670	1087.1	0.3	18.1	81.6	0.0025	1174.4	

Table IV. Compositions and Physical Properties of Ammonium Sulfate-PEG Systems

system	total system				top phase				bottom phase					
	PEG/ (mass %)	salt/ (mass %)	water/ (mass %)	density/ (kg/m ³)	PEG/ (mass %)	salt/ (mass %)	water/ (mass %)	viscosity/ (Pa-s)	density/ (kg/m ³)	PEG/ (mass %)	salt/ (mass %)	water/ (mass %)	viscosity/ (Pa-s)	density/ (kg/m ³)
A	15.0	14.0	71.0	29.6	7.2	63.2	0.0073	1085.9	3.1	19.8	77.1	0.0015	1119.6	
B	18.5	16.0	65.5	41.7	4.6	53.7	0.0136	1090.7	0.5	25.0	74.4	0.0015	1147.4	
C	21.0	20.0	59.0	53.6	2.9	43.6	0.0252	1098.6	0.1	34.1	65.8	0.0017	1184.5	
D	24.0	24.0	52.0	61.2	1.7	37.1	0.0468	1108.1	0.0	40.5	59.4	0.0021	1222.3	
PEG 1000														
E	10.0	14.0	76.0	36.4	3.6	60.0	0.0766	1078.3	0.0	18.6	81.3	0.0012	1102.2	
F	12.0	16.0	72.0	41.9	2.9	55.2	0.1370	1084.7	0.0	21.8	78.2	0.0013	1121.2	
G	14.0	20.0	66.0	52.5	2.1	45.4	0.2850	1094.6	0.0	27.7	72.3	0.0015	1153.0	
H	16.0	24.0	60.0	55.2	1.4	43.4	>0.500	1102.8	0.0	32.6	67.4	0.0018	1187.0	

Table V. Compositions and Physical Properties of Sodium Sulfate-PEG Systems

system	total system				top phase				bottom phase					
	PEG/ (mass %)	salt/ (mass %)	water/ (mass %)	density/ (kg/m ³)	PEG/ (mass %)	salt/ (mass %)	water/ (mass %)	viscosity/ (Pa-s)	density/ (kg/m ³)	PEG/ (mass %)	salt/ (mass %)	water/ (mass %)	viscosity/ (Pa-s)	density/ (kg/m ³)
	A	12.8	9.6	77.6	1082.2	26.6	4.5	68.9	0.0058	1082.2	5.2	13.7	81.1	0.0020
B	10.0	13.0	77.0	1089.9	34.4	2.3	63.3	0.0062	1089.9	2.3	16.2	81.5	0.0018	1162.7
C	11.0	14.0	75.0	1080.7	35.2	2.3	62.5	0.0076	1080.7	1.4	18.3	80.3	0.0019	1182.3
D	12.5	14.5	73.0	1082.4	36.9	1.9	61.3	0.0086	1082.4	0.8	20.3	78.9	0.0018	1192.2
E	14.0	15.0	71.0	1084.2	41.5	1.8	56.7	0.0099	1084.2	0.6	21.6	77.8	0.0019	1203.5
PEG 1000														
F	7.6	9.7	82.8	1076.6	23.6	4.9	71.5	0.0134	1076.6	1.3	12.1	86.7	0.0015	1106.6
G	9.9	10.9	79.2	1075.4	30.8	3.3	65.9	0.0177	1075.4	0.6	14.6	84.9	0.0015	1132.0
H	14.0	10.8	75.3	1079.3	34.9	3.4	61.7	0.0265	1079.3	0.4	16.4	83.2	0.0016	1151.3
I	17.9	12.9	69.3	1085.0	45.1	1.4	53.5	0.0550	1085.0	0.3	21.5	78.3	0.0020	1197.5
PEG 3350														
J	13.0	8.0	79.0	1070.0	25.8	4.3	69.9	0.0442	1070.0	0.5	11.9	87.6	0.0014	1113.2
K	10.0	13.0	77.0	1075.4	36.5	3.2	60.4	0.1160	1075.4	1.4	16.0	82.5	0.0017	1158.5
L	11.0	14.0	75.0	1080.8	38.7	3.1	58.1	0.1420	1080.8	1.1	17.7	81.2	0.0019	1177.5
M	12.5	14.5	73.0	1083.8	40.4	2.9	56.7	0.1780	1083.8	1.1	19.0	79.9	0.0020	1188.4
N	14.0	15.0	71.0	1085.5	41.7	3.2	55.1	0.2060	1085.5	1.2	20.3	78.5	0.0022	1202.6
PEG 8000														

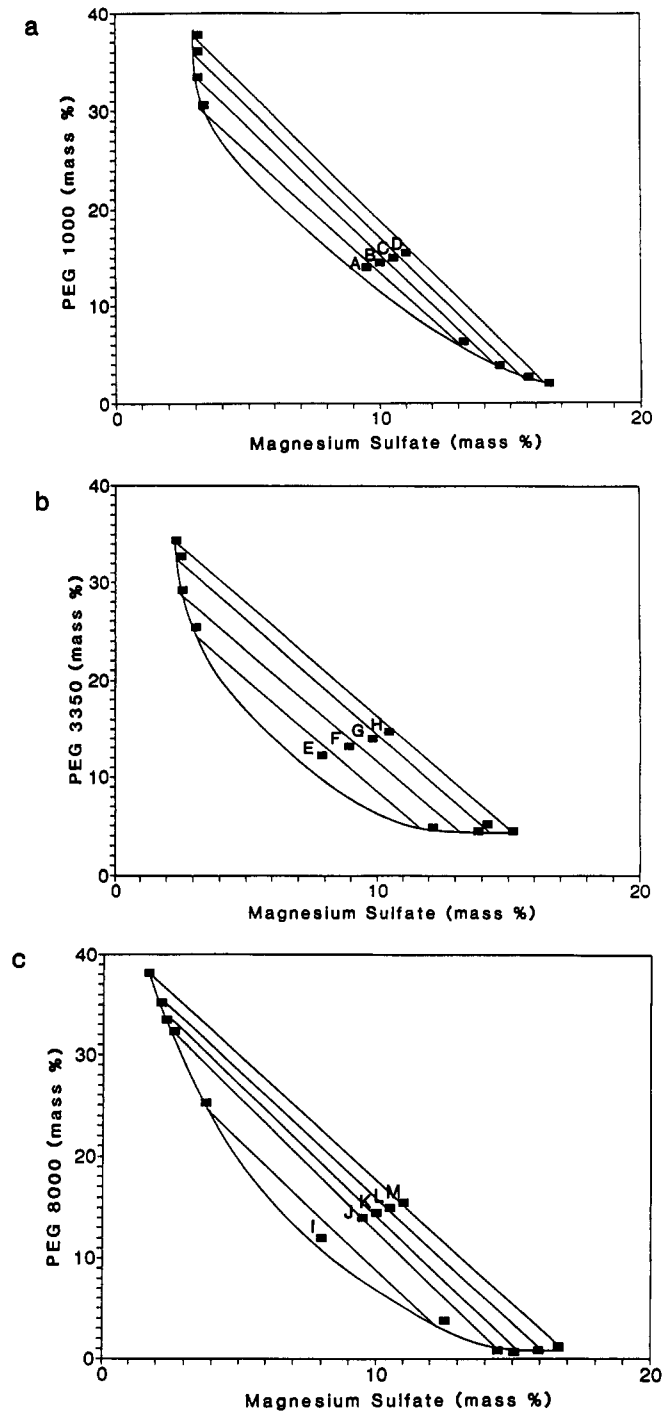


Figure 1. Phase diagrams of magnesium sulfate systems with PEG 1000 (a), PEG 3350 (b), and PEG 8000 (c). The compositions of these systems (A-M) are given in Table I.

compared with analysis via high-performance liquid chromatography (HPLC)-gel permeation chromatography.

Experimental Section

Materials. Three lots of PEG were obtained commercially. The number-average molecular mass (M_n) and the weight-average molecular mass (M_w) were determined using gel permeation chromatography by American Polymer Standards Corp. (Mentor, OH). The columns used were an ultrahydrogel 250 Å and an ultrahydrogel 120 Å in tandem. The mobile phase was water at 1.0 mL/min at 30 °C. The salts used in the phase systems were reagent grade and anhydrous.

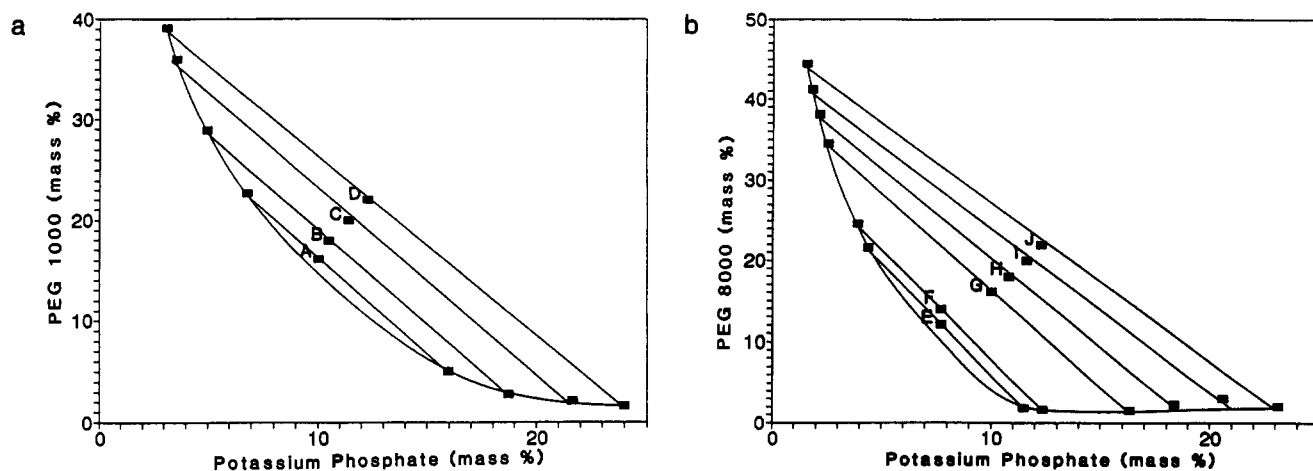


Figure 2. Phase diagrams of potassium phosphate, pH 8.0, systems with PEG 1000 (a) and PEG 8000 (b). The compositions of these systems (A–J) are given in Table II.

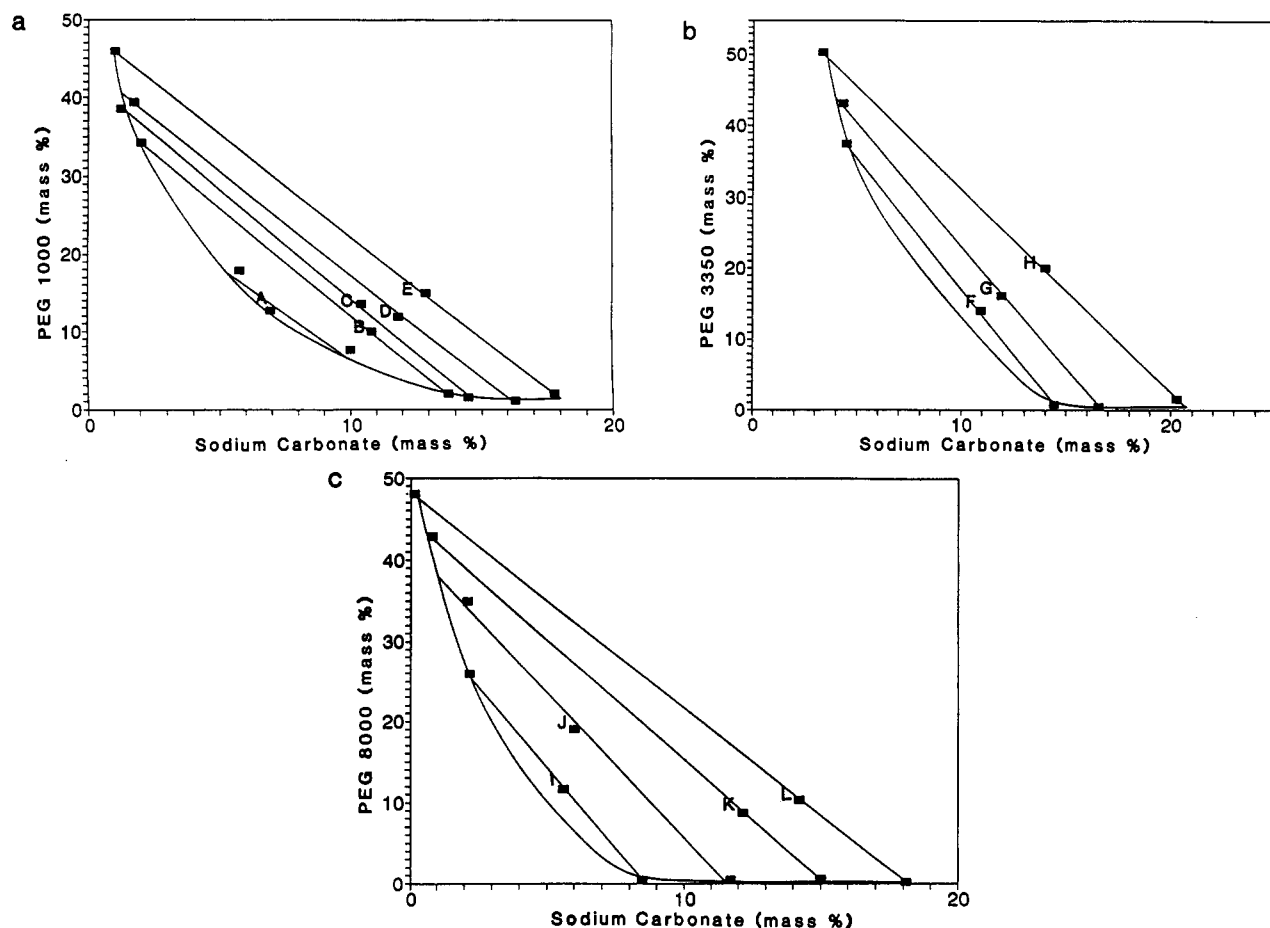


Figure 3. Phase diagrams of sodium carbonate systems with PEG 1000 (a), PEG 3350 (b), and PEG 8000 (c). The compositions of these phase systems (A–L) are given in Table III.

Apparatus and Procedures. ATPS (45 g) were constructed by weighing stock polymer solutions and dry salts into a 50-mL centrifuge tube. For the potassium phosphate systems, the Henderson–Hasselbach equation was used to determine the ratio of mono- and dibasic salts necessary to bring the pH to 8.0. ATPS were brought to 25 ± 0.1 °C in a water bath. The systems were mixed for 2 min each with a vortexer, and then separated at 25 ± 0.5 °C in a centrifuge at 5000g for 10 min, where g is the acceleration due to gravity.

The phase compositions of some of the systems were determined using a gravimetric method. Approximately 100 mg of phase was weighed into a glass tube using an analytical balance reading ± 0.1 mg. Two volumes of water were added, and the solutions were shell frozen in a mixture of dry ice and

acetone. A lyophilizer was used to sublimate the water under a vacuum of <13.3 Pa for 24 h, after which the tubes were again weighed. The sample tubes were placed on the surface of a hot plate at approximately 450 °C for 5 days. The PEG was oxidized and volatilized while the salt remained as a white ash. The tubes were repeatedly weighed until the mass was constant. The estimated reproducibility of the phase compositions was $\pm 0.4\%$ w/w.

The concentrations of salt and PEG in the upper and lower phases of some systems were measured using HPLC–gel permeation chromatography. The column used was a TSK G1000 PW (300 \times 7.5 mm) with a mobile phase of 6.3 mM Na_2HPO_4 and a flow rate of 0.7 mL/min. The PEG and salt were detected using a refractive index detector. Samples were

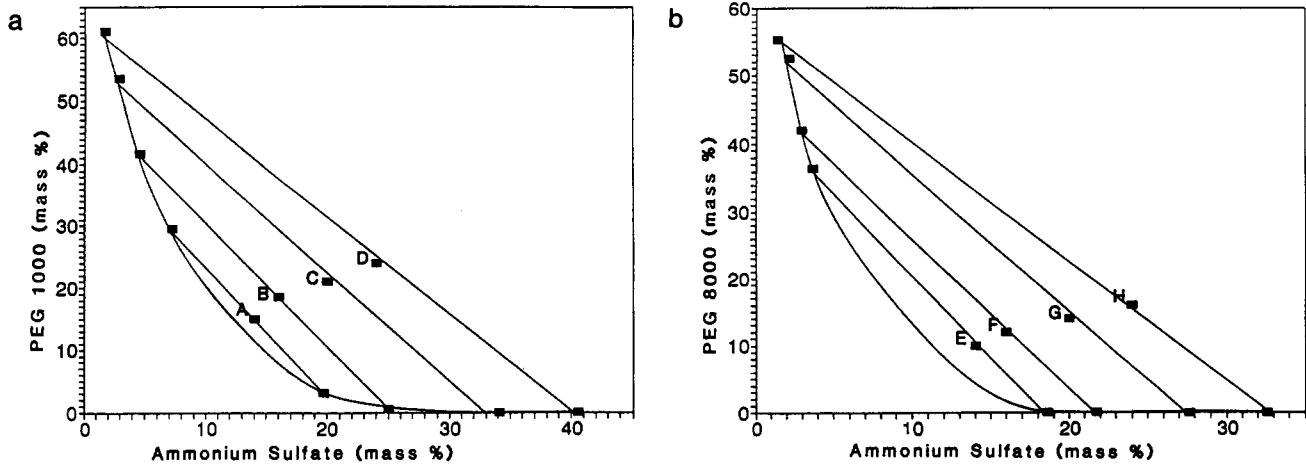


Figure 4. Phase diagrams of ammonium sulfate systems with PEG 1000 (a) and PEG 8000 (b). The compositions of these systems (A–H) are given in Table IV.

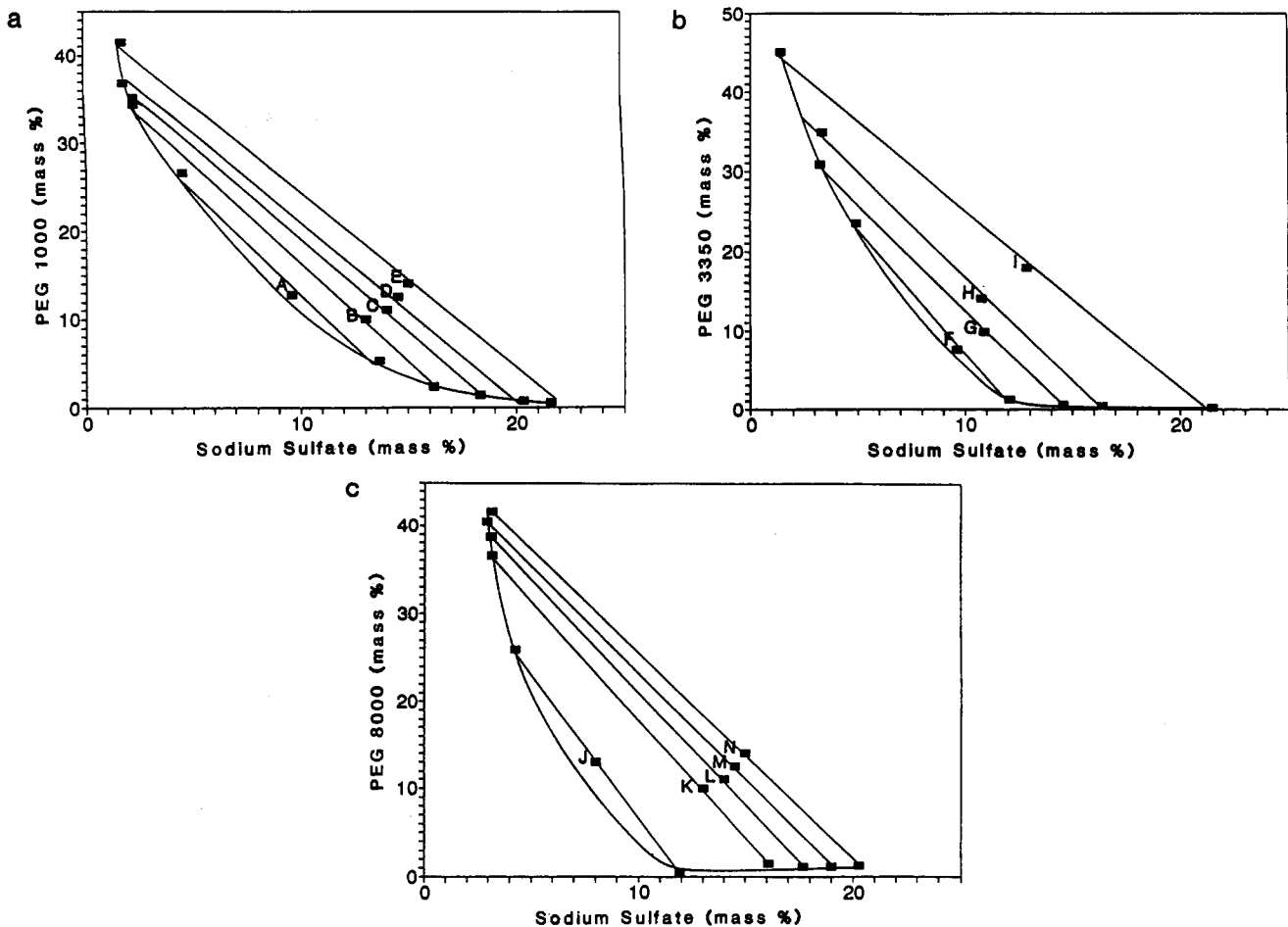


Figure 5. Phase diagrams of sodium sulfate systems with PEG 1000 (a), PEG 3350 (b), and PEG 8000 (c). The compositions of these phase systems (A–N) are given in Table V.

diluted with water so that the integrated area of their peaks fell into the linear range of standard curves generated using PEG 1000, PEG 8000, $(\text{NH}_4)_2\text{SO}_4$, MgSO_4 , and Na_2SO_4 . The phase compositions were reproducible within $\pm 0.4\%$ w/w.

The densities were determined using a vibrating u-tube densitometer with a temperature of 25 ± 0.1 °C. The reproducibility of the densities of the phases was estimated to be ± 0.8 kg/m³. The viscosities were determined using a cone and plate viscometer with a temperature bath of 25 ± 0.1 °C. The viscosities of the separated phases were reproducible within ± 0.0003 Pa·s.

Results and Discussion

The lot of PEG 1000 used in these experiments had an M_n of 1075 and a M_w of 1125 ($M_w/M_n = 1.05$). The PEG 3350 used had an M_n of 3200 and an M_w of 3400 ($M_w/M_n = 1.06$). The PEG 8000 used had an M_n of 8070 and an M_w of 9700 ($M_w/M_n = 1.20$). The densities and viscosities of the phase systems are compiled in Tables I–V. The viscosities generally increase with the increase of PEG molecular mass. The phase densities approach that of water, due to the high water content. In each phase system, both properties tend to increase with

longer tie-line length, with exceptions occurring in the region close to the critical point.

The phase-composition data from Tables I-V are plotted in phase diagrams in Figures 1-5, respectively. The tie lines are determined by connecting each corresponding set of total, bottom, and top phase points. The binodal curve is drawn through the top and bottom phase points, and is estimated near the critical point on the basis of the locations and trends of the top and bottom phase compositions and, in some cases, single phase points.

The phase diagrams with $(\text{NH}_4)_2\text{SO}_4$, MgSO_4 , or Na_2SO_4 combined with PEG 1000 or PEG 8000 were determined using the HPLC method. The remainder of the diagrams were determined gravimetrically. Points from the HPLC data sets were repeated using the gravimetric method. While both methods had virtually the same reproducibility and resulted in values identical within their uncertainty, the gravimetric technique was simpler and less labor intensive.

Literature Cited

- (1) Albertson, P.-A. *Partition of Cell Particles and Macromolecules*, 3rd ed.; Wiley-Interscience: New York, 1986.
- (2) Walter, H.; Brooks, D. E.; Fisher, D. *Partitioning in Aqueous Two-Phase Systems*; Academic Press, Inc.: Orlando, FL, 1985.
- (3) Cabezas, H., Jr.; Kabiri-Badr, M.; Szlag, D. C. *Bioseparation* 1990, 1, 227.
- (4) Edmond, E.; Ogston, A. G. *Biochem. J.* 1968, 109, 569.
- (5) King, R. S.; Blanch, H. W.; Prausnitz, J. M. *AIChE J.* 1988, 34, 1585.
- (6) Kabiri-Badr, M. Ph.D. Thesis, University of Arizona, Tucson, AZ, 1990.
- (7) Szlag, D. C.; Gulliano, K. A.; Snyder, S. M. In *Downstream Processing and Bioseparation*; Hamel, J.-F. P., Hunter, J. B., Sikdar, S. K., Eds.; ACS Symposium Series 419; American Chemical Society: Washington, DC, 1990; pp 71-86.
- (8) Diamond, A. D.; Hsu, J. T.; *Biotechnol. Bioeng.* 1989, 34, 1000.
- (9) Stewart, R.; Todd, P. In *Proceedings from Frontiers in Bioprocessing II*; Sikdar, S., Todd, P., Bier, M., Eds.; ACS Symposium Series; American Chemical Society: Washington, DC, in press.

Received for review July 26, 1991. Revised January 10, 1992. Accepted January 28, 1992.

Anion Exchange in Amberlite IRA-400 and Amberlite IRA-410 Ion Exchange Resins

Modesto López, José Coca, and Herminio Sastre*

Department of Chemical Engineering, University of Oviedo, 33071 Oviedo, Spain

Equilibrium for the binary exchange of anions on Amberlite IRA-400 and Amberlite IRA-410 was measured.

Standard methods were used to determine operating characteristics of both resins. Equilibrium data were obtained by the batch method. The fitting of binary ion exchange isotherm equations is an important aspect of data analysis. The Langmuir, Freundlich, Sips, and Koble-Corrigan isotherms were transformed to a linear form and their adjustable parameters estimated by linear regression. The Langmuir isotherm is the most suitable for both correlation of equilibrium data and prediction and interpretation of breakthrough curves.

Introduction

The three factors that can affect the behavior of an ion exchange column are *equilibrium*, *kinetics*, and *mechanics*. The degree of column efficiency depends primarily on equilibrium (1, 2).

Various methods have been used to obtain binary ion-exchange equilibrium data. The simplest is the *batch method*, proposed by Gregor and Bergman (3).

The dimensionless *equivalent ionic fraction*, x and y , for fluid and solid, respectively, are defined by

$$x = C_1/C_0 \quad y = Q_1/Q$$

where C_1 = concentration of the ion species in the solution, C_0 = total concentration of the solution phase, Q_1 = concentration of the ion species in the solution phase, and Q = total exchange capacity of the resin.

* To whom correspondence should be addressed.

This paper focuses on the study of the anion equilibrium data of the Amberlite IRA-400 and IRA-410 resins fitted to linear transformations of different isotherm equations. The regression coefficients for each resin were determined.

Experimental Section

The resin phase consisted of Amberlite IRA-400 (type I) and Amberlite IRA-410 (type II) gel strong-base anion exchange resins (supplied by Rohm and Haas Co.) in the X-form ($X = \text{CO}_3\text{H}$, Cl , OH , SO_4). Solution phases were mixtures made up using sodium salts of both the X-anion and fluoride anion required to obtain a total concentration of 0.05 N.

The resins were washed with distilled deionized water and regenerated or eluted with 4% sodium sulfate, except in elutions of sulfate ion where 1 N sodium nitrate was used (4).

The resins were conditioned by alternate conversions to the hydroxide and chloride forms and washed until no further chloride could be detected in the effluent. Part of this material was converted into the bicarbonate, chloride, hydroxide, and sulfate forms.

To determine the *water content* of the wet resin, resin samples were put in a Büchner funnel which was connected to a water vacuum pump to remove the interstitial water. After weighing, the resin samples were dried in a desiccator over phosphorus pentoxide to constant weight. The *resin density* was determined in water by a standard-type pycnometer. The *total capacity* for weighed amounts (approximately 5 g) of the ionic form of the resin was determined by adding an excess of sodium salt of X-anions, washing until no further X-anion could be detected in the effluent, regenerating the resin with exactly 1 L each of 4% sodium sulfate (or 1 N sodium nitrate), collecting this effluent in a volumetric flask, and finally determining the X-anion (5-8). Table I shows the physicochemical characteristics of the used resins.

In the *batch equilibrium studies*, weighed amounts (2-3 g) of moist resin were equilibrated with 100 mL of mixtures of